Mechanisms of cooperation and competition of two-species transport in narrow nanochannels

Wolfgang Rudolf Bauer*
Department of Internal Medicine I, University Hospital of Würzburg, Oberdürrbacher Straße 6, D-97080 Würzburg, Germany
(Received 16 June 2017; published 6 December 2017)

Flow of particles of two different species through a narrow channel with solely two discrete spatial positions is analyzed with respect to the species' capability to cooperate or compete for transport. The origin of the latter arises from particle-channel and interparticle interactions within the channel, i.e., blocking the position of a particle, and its interaction with its neighbors in the channel. The variety of occupation options within the channel defines the state space. The transition dynamics within is considered as a continuous Markov process, which, in contrast to mean-field approaches, conserves explicitly spatial correlations. A strong repulsive interaction between particles of the same kind and a very attractive empty channel imply a strong entanglement of transport of both species. In the limiting case of perfect coupling, flows in state space are restricted to a cyclic subspace, where they become all equivalent in the steady state. In particular, this implies equal particle flows of the two species. Entanglement of transport implies that the species mutually exert entropic forces on each other. For parallel directed concentration gradients this implies that the species' ability to cooperate increases with the degree of entanglement. Thus, the gradient of one species reciprocally induces a higher flow of the other species when compared to that in its absence. The opposite holds for antiparallel gradients where species mutually hamper their transport. For a sufficient strong coupling, the species under the influence of the stronger concentration gradient drives the other against its gradient, i.e., the positive mixing entropy production of the driving species becomes the motor for the negative mixing entropy production of the driven one. The degree of effectiveness by which negative entropy production emerges at the cost of positive entropy production increases with the coupling strength. This becomes evident from location and connectivity of the sources of entropy production in state space.

DOI: 10.1103/PhysRevE.96.062109

I. INTRODUCTION

Transport of particles through channels and its regulation is of paramount importance in biological systems as well as in applications in nanotechnology [1,2]. Besides this, the conceptual framework describing channel transport may be easily extended also to describe nonspatial "transport," e.g., along the reaction coordinate of enzymatic reactions.

The transport itself depends on thermodynamic forces, e.g., concentration gradients between the domains connected by the channel, electrical drift forces as well as on particle-channel, and interparticle interactions. In this context, mixed-species transport is of particular interest as the species may mutually affect each others' translocation dynamics inside the channel. Based on a 1D exclusion model [3], Chou [4,5], and Lohse [5] studied solvent-solute transport in a narrow channel connecting baths with different concentrations of the solute. This corresponds to transport of two species, with antiparallel directed concentration gradients, the latter obtained from the respective molar fractions of solute and solvent. The mutual effect on flow varied with the channel-particle binding strength and elongation of the channel, e.g., the latter increased the capability, that one species drives the other against its concentration gradient [4,5]. An intriguing question of mixed-species transport is as follows: under which circumstances do particles of different species with parallel directed concentration gradients cooperate, mutually, at the cost of its own species, promote the other one; or solely compete for transport. This sophisticated behavior was recently shown by us in a simple Markovian model of channel transport [6], which, in contrast to mean-field models, explicitly conserved spatial correlations of interparticle interactions and was numerically exactly solvable. We could demonstrate that the capability for cooperation of the two species increases with the length of the channel.

The origin of the mutual effect of each species on the flow of the other is the interparticle interaction between the species. Due to concentration gradients, the probability of such interactions is distributed asymmetrically within the channel. From this asymmetry, entropic forces emerge which act on particles of one species in the direction of the others concentration gradient. However, interparticle interaction and its implications on flow is janiform. On the one hand, they are the sources of entropic forces by which the species mutually interact, e.g., drive each other. On the other hand, these interparticle interactions hamper flow of either species as a particle blocks its spatial position and thereby its access by other particles.

The yet-unsolved question is as follows: how do the sometimes opposing effects of interparticle interactions and their perhaps complex arrangement affect the coupling of transport of two species? Is there a strategy for choosing interparticle and particle-channel interactions to achieve an optimum coupling? This will be addressed in this paper. Optimum coupling would imply that the thermodynamic driving forces of the species, i.e., the concentration gradient related differences of chemical potentials, would add in their effect on flow of either species. Hence, it is suggestive that an optimum coupling should make the thermodynamic driving forces act in series. The way towards this scenario is made evident in state space, and the transition dynamics, reflected by flows, within. As the approach must hold for the shortest channel which allows interparticle interaction inside, we focus

*Also at: Comprehensive Heart Failure Center, Am Schwarzenberg 15, A15, D-97080 Würzburg, Germany; bauer_w@ukw.de

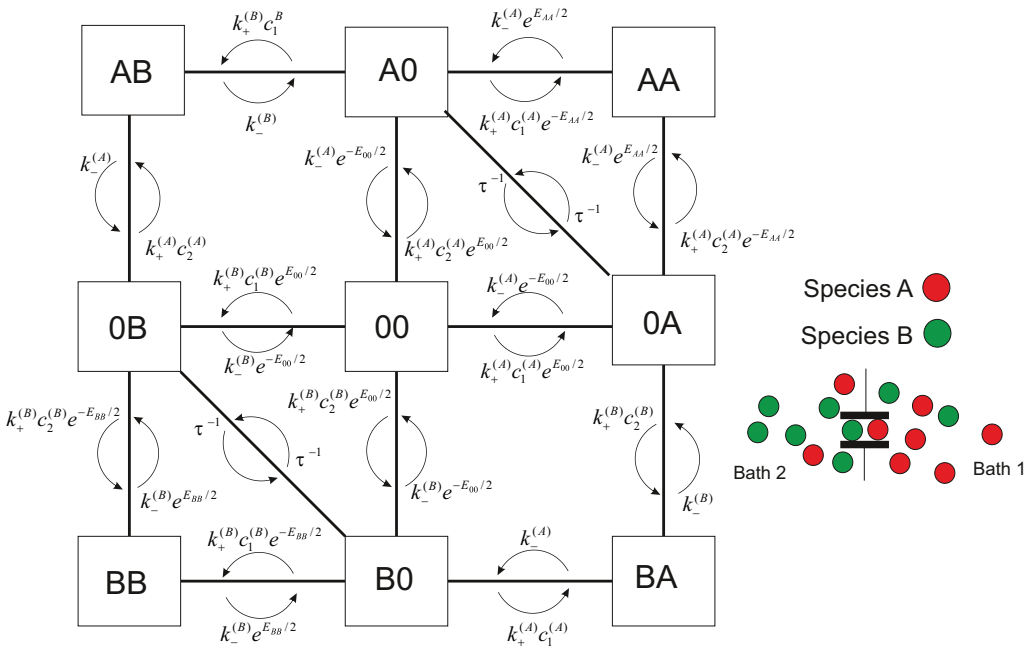

FIG. 1. The nine-dimensional state space $\mathbf{\Sigma} = \{\boldsymbol{\sigma} | \boldsymbol{\sigma} = (\sigma_2, \sigma_1),\ \sigma_i = 0, A, B\}$, with transition rates between states. Right: A sketch of the channel connecting the two baths.

on the minimalist model of a discrete channel with solely two spatial positions inside.

The paper is structured as follows: First, an outline of the model is given, in which we introduce its state space, the Markovian transition dynamics between the states, and the implications for occupation probability and particle flow in the steady state. In the third section we identify which transitions in state space a stochastic path must contain, that it realizes particle transport between the baths. An optimum coupling of transport of the two species implies that these paths must visit certain states and avoid others. This defines the inter- and intraspecies interactions to achieve this optimum coupling. On the way towards optimum coupling of transport, its quality is studied. For parallel-directed concentration gradients, this quality implies the capability of the two species to cooperate, to profit at the cost of the other, or solely to compete for transport. In this context, cooperation means that transport of any species profits from the existence of the other's concentration gradient, whereas sole competition denotes the opposite. Profit at the cost of the other implies that transport of one species is enhanced by the other's gradient, whereas its own gradient hampers flow of the other. In the fourth section it is shown how mixing entropy production of the species is related to its sources, i.e., entropy production related to transitions in state space. This is analyzed as a function of the coupling strength, which measures the degree of entanglement of both transport processes.

II. THE MODEL

Our channel model was recently described in detail [6]. Briefly, the channel connects two baths (1 and 2) with particles of two species $X = A, B$ with respective concentrations, $c_1^{(X)}$, $c_2^{(X)}$, inside. Our minimalist model shall only allow two spatial positions for particles inside the channel, each of which may at most be occupied by only one particle. This implies that any particle transition to a position in the channel demands its vacancy. A channel state is completely described by the state variable $\boldsymbol{\sigma} = (\sigma_2, \sigma_1)$, where the values of σ_i indicate whether the position i is empty ($\sigma_i = 0$) or occupied by a particle of species A ($\sigma_i = A$) or B ($\sigma_i = B$). These states form a $3^2 = 9$-dimensional state space $\mathbf{\Sigma}$ (see Fig. 1).

For simplicity the particle-channel interactions is considered to be homogeneous, i.e., its profile inside the channel is flat. This implies that the transition rates between the two positions are equal, i.e., $r_{(X,0)\to(0,X)} = r_{(X,0)\leftarrow(0,X)}$. In addition, we assume the rates to be the same for the two species. This rate r, which is a measure of the particles mobility in the channel, shall define the time constant $\tau = r^{-1}$, to which we normalized all temporal parameters, i.e.,

$$\tau = r^{-1} = 1. \tag{1}$$

Further, we assume symmetric exchange dynamics of particles at the channel ends with the respective baths. This, and the flat particle-channel interaction profile, imply that particle transport is merely driven by concentration gradients and not by any energetic potential differences between the baths. Hence, the free-energy gain of particles, when passing from the bath with higher particle concentration (e.g., bath 1) to that with the lower one, is determined from the difference of the chemical potentials as [7]

$$\Delta\mu^{(X)} = \ln\left(c_1^{(X)}/c_2^{(X)}\right). \tag{2}$$

Transitions from and to a bath are restricted to respective adjacent channel positions. If we had solely the blocking interparticle interaction, then the transition rate describing the access dynamics from the bath to a vacant channel

position would be proportional to some rate constant k_+ times the particle concentration in the respective bath. In contrast, particles would leave such a position toward the adjacent bath with a rate k_-, where the potential difference $\Delta\Phi = -\ln(k_+/k_-)$ describes the binding strength the channel exerts on the particle [8]. The access of particles from the bath solely requires an empty adjacent channel position and would be independent from the occupation state of the nonadjacent site. However, we now want to consider a more sophisticated interparticle interaction than simple blocking. This can be realized by energetic differences, influencing the bath-channel exchange dynamics, which depend on the occupation state of the nonadjacent channel site. So we introduce an energetic difference, which a particle has to pass on its way from the bath to a vacant spatial position if the channel is already occupied by a particle of the same species X. This, for example, holds for a transition $(0A) \to (AA)$. If $E_{AA} > 0$, then this energetic barrier acts as a repulsive interaction between particles of the same species. The corresponding rates for transitions, i.e., in this case at the left side of the channel, then become [9]

$$\begin{aligned} r_{(0X)\to(XX)} &= k_+ \, e^{-E_{XX}/2} \, c_2^{(X)}, \\ r_{(XX)\to(0X)} &= k_- \, e^{E_{XX}/2}. \end{aligned} \tag{3}$$

The same holds symmetrically for right side of the channel. Bath-channel transitions of particles which enter a channel occupied by a particle of a different species shall solely be described by the rate constants k_+, k_-. We also introduce an energy difference E_{00} describing the affinity of the empty channel ($\boldsymbol{\sigma} = (00)$) to absorb a particle, i.e., this energy is gained when a particle enters an empty channel. These rates are [9]

$$\begin{aligned} r_{(0,0)\to\text{one particle in channel}} &= k_+ \, e^{E_{00}/2} \, c_X, \\ r_{\text{oneparticleinchannel}\to(0,0)} &= k_- \, e^{-E_{00}/2}. \end{aligned} \tag{4}$$

This affinity of the empty channel is assumed to be identical for the two species.

Transition dynamics on the state space is that of a continuous stationary Markov process. The evolution of the probabilities $\boldsymbol{P} = (P_\sigma(t))_{\sigma\in\Sigma}$ to find the channel in the respective states is then determined by a master equation,

$$\frac{d}{dt} \, \boldsymbol{P}(t) = \boldsymbol{\Lambda} \, \boldsymbol{P}(t), \tag{5}$$

with the 3×3 matrix $\boldsymbol{\Lambda} = (\lambda_{\sigma,\varsigma})$ containing the transition rates $\lambda_{\sigma,\varsigma} = \lambda_{\sigma\leftarrow\varsigma}$ from channel states $\boldsymbol{\varsigma}$ to $\boldsymbol{\sigma}$ [10]. They are given by Eqs. (1)–(4) and can be depicted from Fig. 1.

As the system must be in some state, conservation of probability holds, i.e., $d/dt \sum_\sigma P_\sigma = 0$. This determines the diagonal matrix elements of $\boldsymbol{\Lambda}$ as

$$\lambda_{\varsigma,\varsigma} = -\sum_{\substack{\sigma\in\Sigma \\ \sigma\neq\varsigma}} \lambda_{\sigma,\varsigma}. \tag{6}$$

The transition rates between the states $\boldsymbol{\sigma} \leftrightarrows \boldsymbol{\varsigma}$ define a free-energy difference,

$$\Delta\epsilon_{\sigma,\varsigma} = -\ln\left(\frac{\lambda_{\sigma,\varsigma}}{\lambda_{\varsigma,\sigma}}\right), \tag{7}$$

which results either from energetic differences and/or that of entropic forces related to particle exchange. This free-energy differences acts as the driving force for the net flow of probability between the respective states. They are given by

$$J_{\sigma\leftarrow\varsigma} = J_{\sigma,\varsigma} = \lambda_{\sigma,\varsigma} P_\varsigma - \lambda_{\varsigma,\sigma} P_\sigma. \tag{8}$$

With Eq. (6), one can rewrite the master Eq. (5) in the form of a continuity equation of probability,

$$\frac{d}{dt} \, P_\sigma = \sum_{\varsigma\in\Sigma} J_{\sigma,\varsigma}. \tag{9}$$

The latter describes that the change of probability to find the system in state $\boldsymbol{\sigma}$ results from the probability net flows directed to it from all other states $\boldsymbol{\varsigma}$.

When the concentration gradients between the baths vanish, the stationary state of the system is that of thermodynamic equilibrium for which detailed balance holds. Then, all flows between the states in Eq. (8) cease, and the equilibrium probabilities $P^{(e)}$, rates $\lambda^{(e)}$, and corresponding free-energy differences $\Delta\epsilon^{(e)}_{\sigma,\varsigma}$ fulfill the condition

$$P^{(e)}_\sigma / P^{(e)}_\varsigma = \lambda^{(e)}_{\sigma,\varsigma} / \lambda^{(e)}_{\varsigma,\sigma} = e^{-\Delta\epsilon^{(e)}_{\sigma,\varsigma}}. \tag{10}$$

In this case, we can assign the states a potential

$$\phi_\sigma = -\ln\left(P^{(e)}_\sigma\right), \tag{11}$$

i.e., the free-energy differences between states are that between the corresponding potentials

$$\Delta\epsilon^{(e)}_{\sigma,\varsigma} = \phi_\sigma - \phi_\varsigma. \tag{12}$$

This implies that we have a conservative field of driving forces in the state space, i.e., the free-energy difference along a path [start $= \boldsymbol{\sigma}_1 \cdots \boldsymbol{\sigma}_N =$ end] in state space,

$$\sum_{i=1}^{N} \Delta\epsilon^{(e)}_{\boldsymbol{\sigma}_{i+1},\boldsymbol{\sigma}_i} = \phi_{\text{end}} - \phi_{\text{start}}, \tag{13}$$

solely depends on the start and end state of the path. In particular, it vanishes for closed paths.

Nonvanishing concentration gradients of particles between the baths imply a nonconservative field of driving forces on state space, i.e., there exist closed paths in state space in which free energy is gained related to particle transport between the baths. For example, the closed path $[0A - A0 - 00 - (0A)\cdots]$ describes particle transport of species A from bath 1 to bath 2 for which we gain the free energy $\ln(c_1^{(A)}/c_2^{(A)})$. In the following, we want to restrict our study to stationary nonequilibrium conditions, i.e., the system is in its steady state, implying that the probability distribution $\boldsymbol{P}_s$ remains constant in time. Hence,

$$\frac{d}{dt} \, \boldsymbol{P}_s(t) = \boldsymbol{\Lambda} \, \boldsymbol{P}_s \equiv 0, \tag{14}$$

holds, which, with Eq. (9), implies the conservation of flow around any state $\boldsymbol{\sigma}$ (Kirchhoff's cicuit laws)

$$\sum_{\varsigma\in\Sigma} J_{\sigma,\varsigma} = 0. \tag{15}$$

Particle flow between the baths implies flow at the channel ends. For example, flow of species A at the left channel end

(see Fig. 1) results from transitions between the states $(0,\sigma) \leftrightarrows (A,\sigma)$. Hence,

$$J^{(A)} = J_{(0A),(AA)} + J_{(00),(A0)} + J_{(0,B),(AB)}. \tag{16}$$

The conservation of flow in the steady state [see Eq. (15)] then implies that this flow must equal to that within the channel, $J_{(A0),(0A)}$ [note that $J_{(A0),(0A)} = -J_{(0A),(A0)}$], and that at the right channel end $J_{(AA),(A0)} + J_{(0A),(00)} + J_{(BA),(B0)}$. The same holds for species B. Hence, we obtain for particle flow between the baths

$$J^{(A)} = J_{(A0),(0A)} \text{ and } J^{(B)} = J_{(B0),(0B)}. \tag{17}$$

In the following we determine steady-state probabilities from Eq. (14) numerically and from this the flows between the states [Eq. (8)] and of particles through the channel [Eq. (17)].

III. COOPERATION AND COMPETITION

Within the state space our system undergoes stochastic transitions according to the master Eq. (5). The net thermodynamic driving forces for particle transport across the channel are the concentration gradients of particles between the respective baths. A nonvanishing net particle transport of species X ($X = A, B$), e.g., from bath 1 to bath 2, requires the repetitive visit of the states $(0X)$ and $(X0)$ [Eq. (17)]. So the stochastic path of successive states may be built up from closed paths which contain the segment $(0X)-(X0)$. The entanglement of the species' transport should mainly depend on the options particles have to interact within the channel. In order to realize this interaction, our minimalist channel model with only two spatial positions inside offers solely two states, (AB) and (BA). Hence, interparticle interactions and particle channel interactions which favor visits to these states, or, vice versa, which hamper access to states that are not involved in paths leading to these two states, should favor cooperation or competition. So, entanglement of different species' transport is realized on closed paths which contain the segments $(0A)-(A0)$ and $(0B)-(B0)$ as well as the states (AB) and (BA). However, cooperation and competition do not merely depend on the presence of states in which different species coexist in the channel. Instead, being in these states, the species must mutually exert some force on each other. Here, it is an entropic force which results from the left-right bias of occupation inside the channel, which itself results from the concentration gradients.

For simplicity, from now on in this paper, we set the affinity of the empty channel E_{00} to attract any particle and the repulsive interaction energies E_{AA}, E_{BB}, impeding occupation of the channel by particles of the same species, equal and define this new energetic quantity

$$\Delta E = E_{00} = E_{AA} = E_{BB} \tag{18}$$

as the coupling strength with which transport of the two species are entangled. Obviously, a high coupling strength favors transition to channel states occupied by a single particle of any species inside as well as to states occupied by different species. According to the previous paragraph, the first are a prerequisite for transport and the second for interaction of both species. The significance of this will become evident in the following.

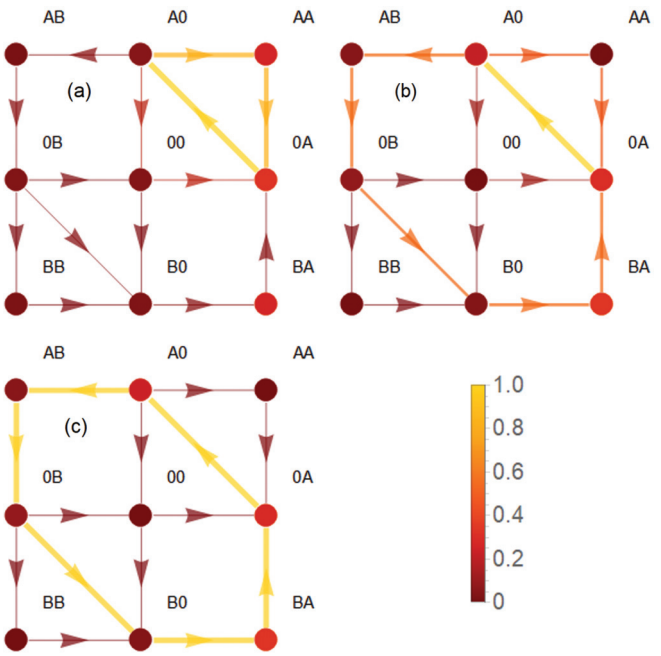

FIG. 2. Flows and occupation probabilities in state space. Different energetic levels of the empty channel state and channel states occupied by two particles of the same species are considered. For simplicity, all are set equal to $\Delta E = E_{00} = E_{AA} = E_{BB}$, i.e., the coupling strength quantifying entanglement of transport of the two species [see Eq. (18)]; $\Delta E = 0$ (a), $\Delta E = 7$ (b), and $\Delta E = 15$ (c). Values for probabilities are color coded (see bar). So are flow values, which were normalized to that with the maximum magnitude. In addition, flow magnitude is coded by the thickness of the arrows, which indicate the flow direction. Particle concentrations of species A in the right (1)and left (2) bath are $c_1^{(A)} = 10$ and $c_2^{(A)} = 0.1$, respectively. $k_+^{(A)}$ and $k_-^{(A)}$ were set equal to 1. Concentrations of B were set equal in both baths, and jump-in rates were chosen to be $k_+^{(B)} c_i^{(B)} = e^1 \times 0.1$, $i = 1, 2$ and jump-out $k_-^{(B)} = e^{-1}$. This choice of rates implied a moderate attractive particle-channel interaction $\Delta\Phi^{(B)} = -\ln(k_+^{(B)}/k_-^{(B)}) = -2$ for species B compared with that of A, $\Delta\Phi^{(A)} = -\ln(k_+^{(A)}/k_-^{(A)}) = 0$. Note that with increasing ΔE, flow is mainly present on the cyclic state space CS (yellow color) (19).

The second law of thermodynamics favors paths in which free energy is gained. In the steady state this translates into the direction and magnitude of stationary flows between states [see Eq. (8)]. From this flow pattern one can infer which paths are favored. In Fig. 2 a concentration gradient drives particles of species A from bath 1 to bath 2. Concentration of species B was chosen to be equal in both baths, i.e., transport of the latter solely depends on its interaction with species A. For the native set up, i.e., for a vanishing coupling strength, which implies an indifferent affinity of the empty channel to attract particles, nor a repulsive interaction impeding occupation by particles of the same species, $\Delta E = E_{00} = E_{AA} = E_{BB} = 0$, the most favored cyclic path is $(0A) - (A0) - (AA) - (0A) \cdots$ [Fig. 2(a)]. On this path the free energy,

$$-(\Delta\epsilon_{(A0),(0A)} + \Delta\epsilon_{(AA),(A0)} + \Delta\epsilon_{(0A),(AA)}) = \ln\left(\frac{c_1^{(A)}}{c_2^{(A)}}\right) = \Delta\mu^{(A)},$$

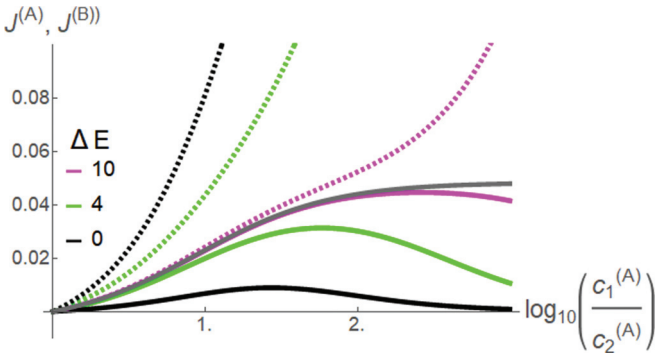

FIG. 3. Particle flow of species A (dashed lines) and B (solid lines) through the channel as a function of the concentration gradient of A. Particle concentration in bath 1 is elevated and that in bath 2 is held constant ($k_+^{(A)} c_2^{(A)} = 0.1$). Concentrations of B are equal in both baths. These and the constants k_+, k_- for both species are identical with that in Fig. 2. The interaction between the species, i.e., entanglement of respective transports, is varied by the coupling strength ΔE of Eq. (18). The gray line gives the flow $J^{\rm cs}$ in the cyclic state space CS (19) and is obtained from Eq. (21). Note that the flows of A and B converge towards this flow with increasing ΔE.

is gained. Only a negligible fraction of flow passes through the states (AB), (BA), and, hence, particle flow of B, which according to Eq. (17) is identical with that from $(0B)$ to $(B0)$, is only moderate [see Fig. 2(a) and the black solid line in Fig. 3]. Figure 2 shows that with increasing coupling strength ΔE, closed paths including the states (AB) and (BA) become more favorable. As a result, the flow of the driven species B increases, whereas that of the driving species A decreases (Fig. 3). In the limiting case for extreme high coupling ($\Delta E \to \infty$) visitations of states, and hence flow between them, is reduced to those belonging to the cyclic state space CS [Fig. 2(c)],

$$(0A) - (A0) - (AB) - (0B) - (B0) - (BA) - (0A) - (0A) \cdots . \tag{19}$$

As this cyclic substate space has no branching, all flows between connected states are equal in the steady state. In particular, particle flows of species A and B are equal in this limiting case, i.e.,

$$\lim_{\Delta E \to \infty} J^{(A)}(\Delta E) = \lim_{\Delta E \to \infty} J^{(B)}(\Delta E) = J^{\rm cs}, \tag{20}$$

which is shown in Fig. 3. Here, with increasing ΔE, the flows of both species converge towards $J^{\rm cs}$. In general, this steady-state flow of a circular Markov process is obtained as (see Appendix A)

$$J^{\rm cs} = \frac{1 - e^{\Delta U}}{\tau_+ + e^{\Delta U}\, \tau_- + R} \tag{21}$$

with ΔU as the free-energy difference the system experiences after one turn in the CS. It is obtained from the single free-energy differences [Eq. (7)] between successive states $\boldsymbol{\sigma}_{i+1}$, $\boldsymbol{\sigma}_i$ in CS [see scheme (19)] as

$$\begin{aligned} \Delta U &= \sum_{i=1}^{5} \epsilon_{\boldsymbol{\sigma}_{i+1}, \boldsymbol{\sigma}_i} = -\ln\left[\frac{c_1^{(A)}}{c_2^{(A)}}\right] - \ln\left[\frac{c_1^{(B)}}{c_2^{(B)}}\right] \\ &= -\Delta\mu^{(A)} - \Delta\mu^{(B)}, \end{aligned} \tag{22}$$

i.e., $|\Delta U|$ is the sum of the chemical potential differences of both species. τ_+ and τ_- are the mean first passage times one needs to pass one turn in the CS in the counterclock (+) or clockwise (−) direction. The starting state may be chosen arbitrarily [11]. R^{-1} is the conductivity of probability flow on CS. For explicit determination of the stead-state flow in CS, first passage times, and conductivity, see Appendix A.

In CS there is maximum entanglement of transport of both species. The equivalence of flows of the two species [Eq. (20)] implies that the thermodynamic driving force, i.e., the concentration gradient, of any species acts equally on flow of both species. When the chemical potentials of both species have the same sign, i.e., the concentration gradients are parallel, they add synergistic to a greater driving force [Eq. (22)]. In Appendix B we show that an increase of the chemical potential of either species by raising its higher concentration always increases flow on the CS. Hence we have a perfect cooperation, as an increase of the concentration gradient of either species increases equally flow of both. Note that this is not as trivial as it may appear at a first glance. Increasing the higher concentration of any species could also imply that blocking reduces flow of the other species. When concentration gradients are antiparallel directed, i.e., the corresponding chemical potentials have opposite signs, reducing the magnitude of the whole driving force $|\Delta U|$ reduces flow of either species until both cease for vanishing ΔU.

The way towards this extreme coupling of transport of both species and, hence, their capability to cooperate is shown in Fig. 4 for parallel-directed concentration gradients. We define cooperation when flow of either species mutually profits from an existing parallel-directed concentration gradient of the other, i.e.,

$$\begin{aligned} J^{(A)}[\Delta\mu^{(A)}, \Delta\mu^{(B)}] &> J^{(A)}[\Delta\mu^{(A)}, 0] \\ J^{(B)}[\Delta\mu^{(A)}, \Delta\mu^{(B)}] &> J^{(B)}[0, \Delta\mu^{(B)}]. \end{aligned} \tag{23}$$

Opposite competition at the cost of both implies that flow of either species decreases in the presence of a parallel-directed gradient of the other species when compared to a vanishing gradient. Promotion of one species at the cost of the other, e.g., B at the cost of A, is given when the parallel-directed gradient of the latter induces a higher flow of B compared to a vanishing gradient; however, flow of A is reduced by the gradient of B,

$$\begin{aligned} J^{(B)}[\Delta\mu^{(A)}, \Delta\mu^{(B)}] &> J^{(B)}[0, \Delta\mu^{(B)}] \\ J^{(A)}[\Delta\mu^{(A)}, \Delta\mu^{(B)}] &< J^{(A)}[\Delta\mu^{(A)}, 0]. \end{aligned} \tag{24}$$

In contrast, we reverse the greater-than and less-than signs when A is promoted at the cost of B. The phase diagrams in

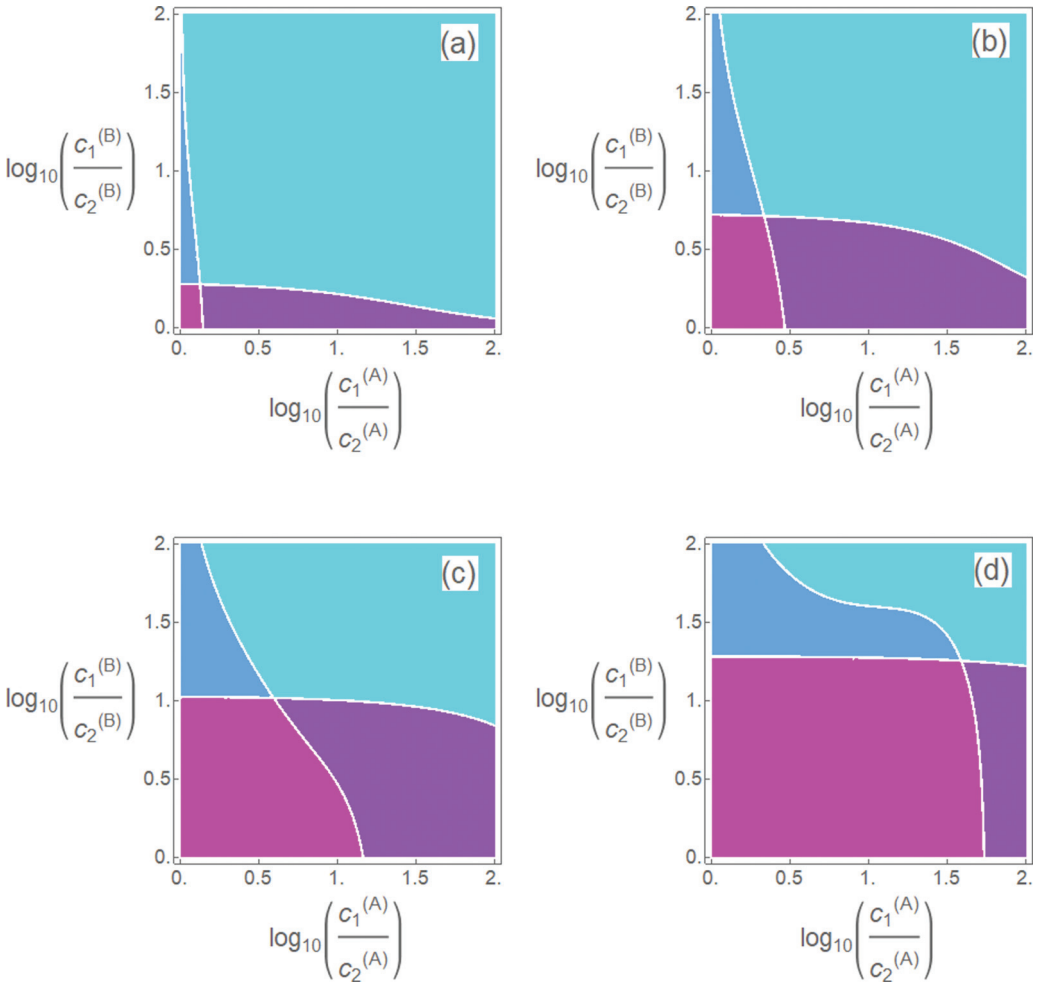

FIG. 4. Phase diagram showing cooperation, promotion, and competition of two-species particle transport as a function of their coupling strength, quantified by ΔE [Eq. (18)]; $\Delta E = 0$ (a), $\Delta E = 2$ (b), $\Delta E = 3$ (c), and $\Delta E = 4$ (d). Concentrations in the left bath (2) were held constant at $k_+^{(A)} c_2^{(A)} = 0.1$ and $k_+^{(B)} c_2^{(B)} = e^1 \times 0.1$, whereas concentrations in the right bath (1) were elevated. The other parameters are identical with those in Fig. 2. Pink denotes cooperation with profit for both, turquoise competition at the cost of both, violet shows that species B is promoted by A at the cost of the latter and vice versa in blue (see text).

Fig. 4 show that with increasing entanglement of the transport pathways of the two species (ΔE increases) the range of concentration gradients, for which both cooperate, increases (pink), whereas those of lossy competition (turquoise) decreases. In the limiting case ($\Delta E \to \infty$) there would be sole cooperation as state space is reduced to CS.

The dependence of species transport on the degree of entanglement also holds for opposing concentration gradients. In the extreme case, when there is a perfect coupling of transport in the CS, flows of both vanish for opposing but equal-magnitude concentration gradients [$\Delta\mu^{(A)} = -\Delta\mu^{(B)}$], as there is no net driving force left. This become evident in Fig. 5, where the gradient of species A is held constant and that of B in opposing direction increases. For a vanishing gradient of B, the gradient of A drives B parallel to its direction ($J^{(B)} > 0$). Flow of B is positively related to the coupling strength. Increasing an opposing gradient of B [$\Delta\mu^{(B)} = \log(c_1^{(B)}/c_2^{(B)}) < 0$] monotonically decreases flow of B until cessation and changes its sign parallel to that of its gradient. This procedure also decreases flow of species A. The stronger the coupling, the higher must be the opposing gradient of B to achieve cessation of its flow. For for strong coupling, $\Delta E = 20$, the flow curves of species A and B become almost

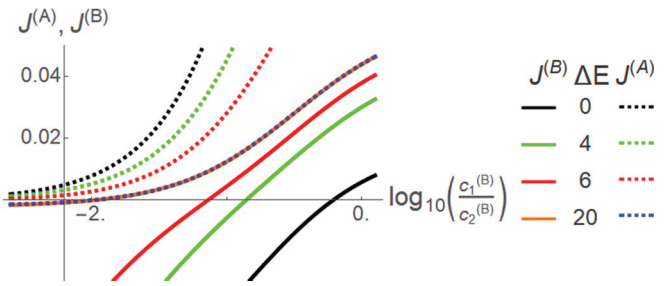

FIG. 5. Effect of opposing concentration gradient of species A and B on respective flows as a function of the coupling strength ΔE. Concentrations and jump-in and -out rates for species A are that from Fig. 2, i.e., the concentration gradient is directed from bath 1 to bath 2, with $c_1^{(A)}/c_2^{(A)} = 100$. Concentration of B in bath 1 is held constant at $k_+^{(B)} c_1^{(B)} = e^1 \times 0.1$, and $c_2^{(B)}$ is increased. The stronger the coupling the higher must be the oppositely directed gradient of B to make its flow cease.

identical (dotted blue and solid orange lines in Fig. 5), and both flows cease for equal opposing concentration gradients $c_1^{(B)}/c_2^{(B)} = c_2^{(A)}/c_1^{(A)} = 10^{-2}$.

IV. ENTROPY PRODUCTION

To evaluate the thermodynamic coupling of two-species transport, the entropy production related to state-space transitions will be determined. In general entropy production of a system which is coupled by heat or particle exchange to baths consists of entropy production within its state space $\mathbf{\Sigma}$, which can be measured by changes of the Shannon entropy,

$$S_{\mathbf{\Sigma}} = \sum_{\boldsymbol{\sigma}\in\mathbf{\Sigma}} -\ln(P_{\boldsymbol{\sigma}})P_{\boldsymbol{\sigma}}, \tag{25}$$

with probability $P_{\boldsymbol{\sigma}}$ to find the system in the state $\boldsymbol{\sigma}$, and the entropy production within the baths $\dot{S}_{\text{bath}}$, i.e.,

$$\dot{S} = \dot{S}_{\mathbf{\Sigma}} + \dot{S}_{\text{bath}}. \tag{26}$$

The latter refers to Schnackenberg's entropy production [12], which is the sum of particular entropy productions in the baths resulting from transitions between the states of the system. For example, for transitions between the two states $\boldsymbol{\sigma} \leftrightarrows \boldsymbol{\varsigma}$, it is determined by the corresponding flow $J_{\boldsymbol{\sigma},\boldsymbol{\varsigma}}$ and the free-energy difference $\Delta\epsilon_{\boldsymbol{\sigma},\boldsymbol{\varsigma}}$ [see Eqs. (7) and (8)] between the states, obtained in direction of the flow, i.e.,

$$\dot{S}_{\boldsymbol{\sigma},\boldsymbol{\varsigma}} = -\Delta\epsilon_{\boldsymbol{\sigma},\boldsymbol{\varsigma}} J_{\boldsymbol{\sigma},\boldsymbol{\varsigma}}. \tag{27}$$

The latter equation is easily understood, e.g., when $\Delta\epsilon$ is an energetic difference, Eq. (27) describes the heat production per time in the bath. When $\Delta\epsilon$ is related to particle exchange, it is a step within the mixing entropy process. Note that a prerequisite for application of Eq. (27) is the assumption of instantaneous equilibration of heat (thermostatted) and/or particle concentrations within the baths. As we consider steady-state conditions, the Shannon entropy within state space in Eq. (25) remains constant. Hence, the whole entropy production reduces to

$$\dot{S} = \frac{1}{2}\sum_{\boldsymbol{\sigma},\boldsymbol{\varsigma}\in\mathbf{\Sigma}} \dot{S}_{\boldsymbol{\sigma},\boldsymbol{\varsigma}}. \tag{28}$$

The factor $1/2$ derives from the fact that $\Delta\epsilon_{\boldsymbol{\sigma},\boldsymbol{\varsigma}}$, and $J_{\boldsymbol{\sigma},\boldsymbol{\varsigma}}$ change concordant signs, when states $\boldsymbol{\sigma}$ and $\boldsymbol{\varsigma}$ are interchanged, i.e., $\dot{S}_{\boldsymbol{\sigma},\boldsymbol{\varsigma}} = \dot{S}_{\boldsymbol{\varsigma},\boldsymbol{\sigma}}$. As shown in the Appendix C, the entropy production in Eq. (28) is equivalent to the sum of the mixing entropy productions $\Delta\mu^{(X)}J^{(X)}$, $X = A,B$ in the baths, i.e., we have

$$\dot{S} = \Delta\mu^{(A)}J^{(A)} + \Delta\mu^{(B)}J^{(B)}. \tag{29}$$

Conversely, this equation states that mixing entropy production by channel transport has its sources in entropy productions resulting from transitions in state space.

In Fig. 6, opposing concentration gradients determine particle transport from bath 1 to bath 2 for species A and, vice versa, for species B. For a moderate coupling of the transport pathways of the two species [$\Delta E = 5$, Fig. 6(a)], respective flows are parallel with the direction of their concentration gradients, i.e., from bath 1 to bath 2 for species A, as reflected by flow $(0A) \to (A0)$ and, vice versa, for species B from bath 2 to bath 1 as shown by flow $(0B) \leftarrow (B0)$. The loose coupling enables that each species follows its thermodynamic driving force and is not much affected by that of the other species. The preferred closed paths in state space which are involved in particle transport between the baths are $(0A) \to (A0) \to (AA) \to (0A)\cdots$ for species A and $\cdots(0B) \leftarrow (B0) \leftarrow (BB) \leftarrow (0B)$ for species B, respectively. Note that the higher flow of species B when compared to that of A is induced by its attractive particle channel interaction $\Delta\Phi^{(B)} = -\ln(k_+^{(B)}/k_-^{(B)}) = -2$. Closed paths including the empty channel state (00) are less frequented. Entropy production is negative for transitions $(0B) \to (BB)$, and $(A0) \to (AA)$. This is due to the fact that these transitions require heat from the baths as the states (AA) and (BB) are on a higher energetic level when compared to their initial state, $\Delta E = 5$ for A and $\Delta E + \Delta\Phi^{(B)} = 5 - 2 = 3$ for B. This fraction of entropy production related to purely energetic transitions cannot be compensated by that related to particle exchange. However, the purely energetic component of negative entropy production is exactly balanced by a positive entropy production when particles are set free towards the baths in direction of their gradient, i.e., $(BB) \to (B0)$ and $(AA) \to (0A)$. The fraction of entropy production solely related to particle exchange is, in contrast, always positive around the states occupied by two like particles.

With increasing coupling [$\Delta E = 10$, Fig. 6(b)], flow towards states occupied by two unlike particles is favored at the cost of flow towards states with two like particles. The entropy production is still similar to the situation with $\Delta E = 5$; however, there emerges a negative, particle-exchange related entropy production for the species B involved flows $(A0) \to (AB)$ and $(BA) \to (0A)$. This is due to the fact that these flows form a fraction of overall flow of B between the baths which is directed from bath 1 to bath 2, i.e., antiparallel to the thermodynamic driving force of B. However, overall flow of B is, at this coupling strength, still parallel to its driving force, i.e., $(0B) \leftarrow (B0)$.

For a strong coupling strength [$\Delta E = 20$, Fig. 6(c)], flow is almost solely present on the cyclic state space CS (19), where it is constant throughout. As flow towards states occupied by two like particles has almost ceased, entropy production consists solely of its particle exchange related component. The negative entropy production related to flows between states $(A0) \to (AB)$ and $(BA) \to (0A)$ is now in series with positive entropy production induced by flows between $(AB) \to (0B)$ and $(B0) \to (BA)$. The negative entropy production is related to transport of B against its gradient, the positive entropy production, which acts as the thermodynamic motor for this process, driveing A in the direction of its concentration gradient. The sum of both must be positive, i.e., the whole mixing entropy production in the baths [Eq. (29)], is positive, which satisfies the second law of thermodynamics.

Figure 7 shows how the mixing entropy production of species B depends on its concentration gradient, the direction of which is opposed to that of the driving species A and the coupling parameter ΔE. Entropy production is zero for a vanishing gradient of B, $c_2^{(B)} = c_1^{(B)}$. Increasing this opposed gradient of B makes the mixing entropy production become

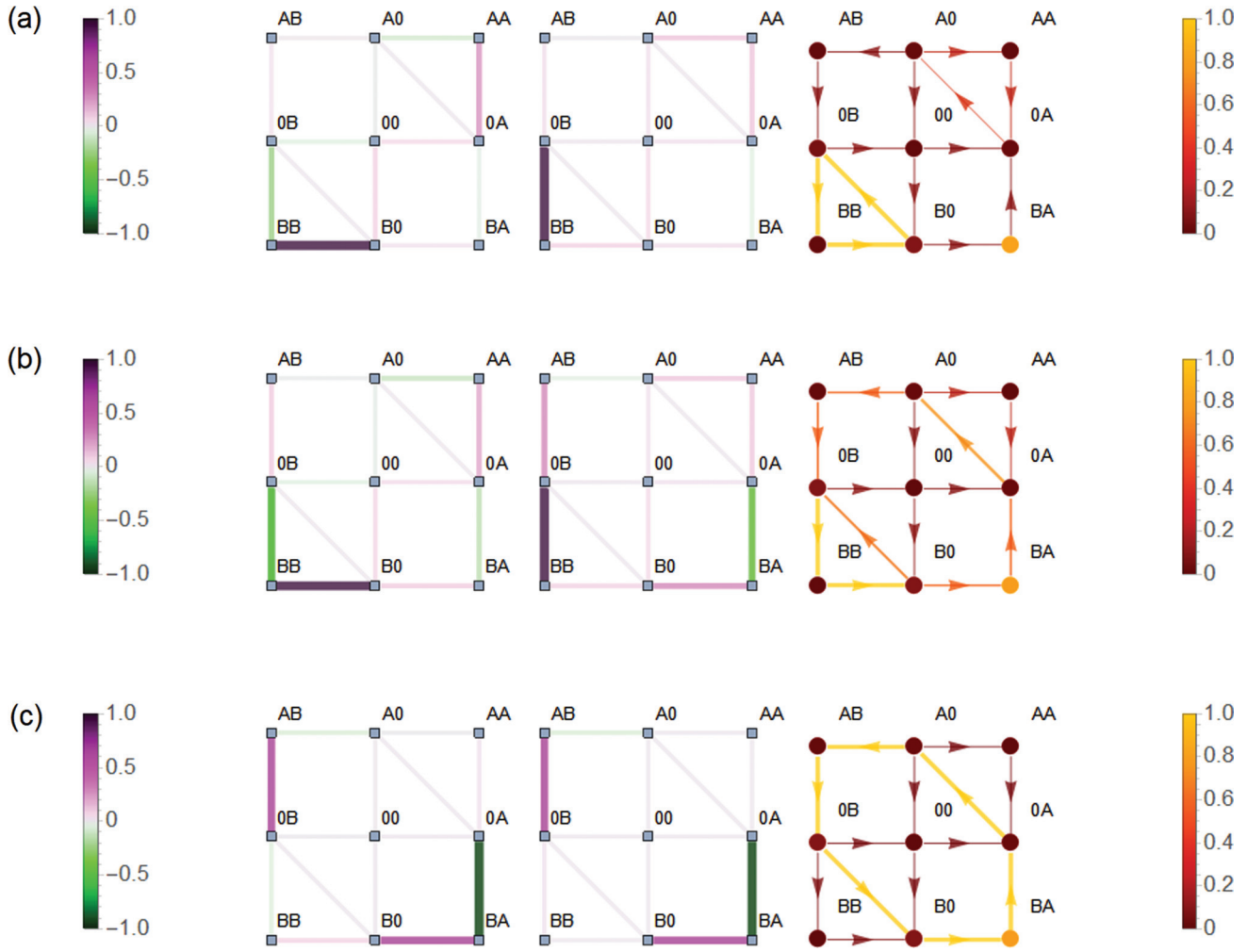

FIG. 6. Entropy production (left panel), entropy production related to particle exchange (mid panel), and flow with occupation probability (right panel) in state space as a function of the coupling strength ΔE [see Eq. (18)]. $\Delta E = 5$ (a), $\Delta E = 10$ (b), and $\Delta E = 20$ (c). The values of entropy production are normalized to their maximum magnitude ($\to \dot{S}_{\sigma,\varsigma}/\mathrm{Max}(|\dot{S}_{\sigma,\varsigma}|)$ and color coded from -1 to $+1$ (left color bar). Coding of flow and occupation probability (0 to $+1$, right color bar) is identical with that in Fig. 2. Concentration gradients of A and B are opposite, $c_1^{(A)}/c_2^{(A)} = 100$, $c_2^{(B)}/c_1^{(B)} = 50$, with $k_+^{(A)}c_2^{(A)} = 0.1$, $k_-^{(A)} = 1$ and $k_+^{(B)}c_1^{(B)} = e^1 \times 0.1$, $k_-^{(B)} = e^{-1} \times 1$, the latter implying a moderate attractive particle-channel interaction $\Phi^{(B)} = -\ln(k_+^{(B)}/k_-^{(B)}) = -2$. Note that for loose coupling (a) flows of both species between the baths follow the direction of their gradient, i.e., they are opposite, $(0A) \to (A0)$ vs. $(0B) \leftarrow (B0)$. A strong coupling (c) almost restrains the transition dynamics of the system to the CS (19) in which directions of particle flows are parallel $(0A) \to (A0)$ and $(0B) \to (B0)$.

negative as flow and gradient of B are antiparallel directed. Eventually, the mixing entropy production of B reaches a minimum before it vanishes when the concentration gradient of B is strong enough to make the flow of B cease, i.e., when it balances the driving effect of A. An increasing coupling strength increases this "ceasing" gradient of B and for $\Delta E \to \infty$ the corresponding thermodynamic driving force approaches that of A, i.e., $|\Delta\mu^{(B)}_{\mathrm{cease}}| \to |\Delta\mu^{(A)}|$. The reason is that an increasing coupling strength confines the relevant state space to the CS (19). Within this cyclic state space the free-energy gain, $\Delta\mu^{(A)}$, and loss, $\Delta\mu^{(B)}$, are in series [see Eq. (22)]. Flows of B and A become identical [Eq. (20)], i.e., both cease when the opposed gradients have the same magnitude, $\Delta\mu^{(B)} = -\Delta\mu^{(A)}$. The efficiency of A to drive B against its gradient, i.e., its capability to create negative entropy production for B by pumping it against its gradient at the cost of its own positive entropy production $\dot{S}^{(B)}/\dot{S}^{(A)}$, increases with the coupling strength [Fig. 7(b)]. For strong coupling, flows of A and B become equivalent [Eq. (20)] and the efficiency approaches

$$\eta = \lim_{\Delta E\to\infty} \frac{\dot{S}^{(B)}}{\dot{S}^{(A)}} = \frac{\Delta\mu^{(B)}}{\Delta\mu^{(A)}} \underbrace{\lim_{\Delta E\to\infty} \frac{J^{(B)}}{J^{(A)}}}_{J^{(A)},\ J^{(B)}\to J^{(\mathrm{cs})}} = \frac{\Delta\mu^{(B)}}{\Delta\mu^{(A)}} . \quad (30)$$

This reflects, that, for a strong coupling strength, the magnitude of the efficiency increases with the gradient of the driven species or, more precisely, with the magnitude of its chemical potential difference. In this regime, all the thermodynamic driving force of species A may be used to drive B against its oppositely directed gradient, until the latter approaches that of A, which makes flow of all species, and hence also mixing entropy productions, vanish.

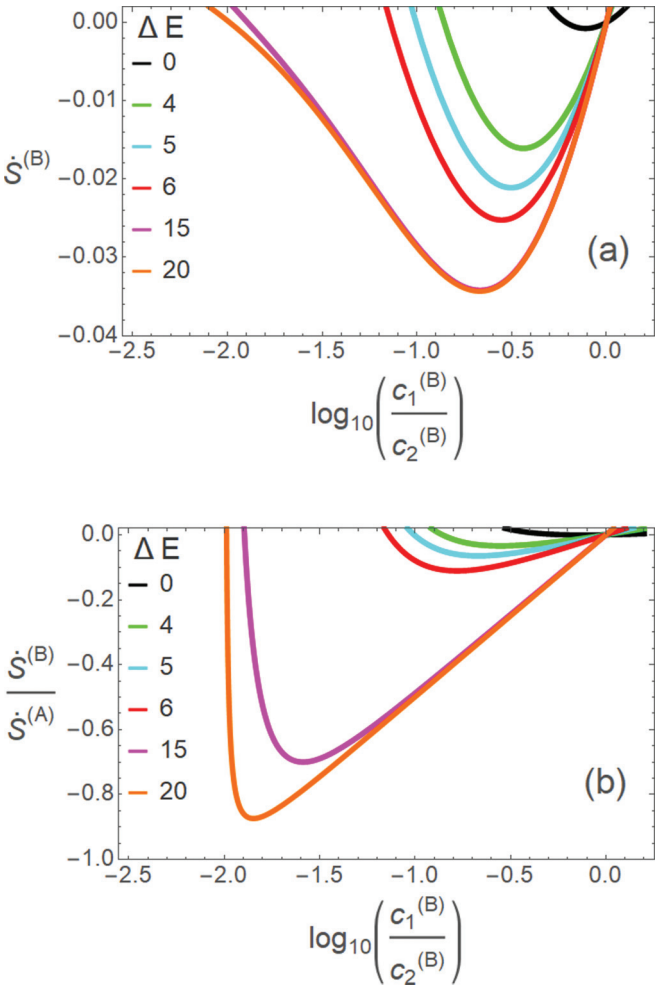

FIG. 7. (a) Negative mixing entropy production of species B, $\dot{S}^{(B)} = \Delta\mu^{(B)} J^{(B)}$. The negative sign is due to transport of B in an antiparallel direction to its concentration gradient. (b) The corresponding efficiency which is defined by the negative entropy production of B per positive entropy production related to transport of A. The concentration gradient of A is directed from bath 1 (right) to bath 2 (left), $c_1^{(A)}/c_2^{(A)} = 100$, with $k_+^{(A)} c_2^{(A)} = 0.1$. Particle concentration of B in bath 1 is set to $k_+^{(B)} c_1^{(B)} = e^1 \times 0.1$ and that in bath 2 is elevated about this level to induce an opposing gradient to that of species A. Jump-out rates at the channel ends of both species are as in Fig. 6. Various coupling strengths ΔE are considered. With maximum coupling strength the efficiency curve (orange line) approaches $\dot{S}^{(B)}/\dot{S}^{(A)} \approx \Delta\mu^{(B)}/\Delta\mu^{(A)} = \ln(c_1^{(B)}/c_2^{(B)})/\ln(c_1^{(A)}/c_2^{(A)}) = \log_{10}(c_1^{(B)}/c_2^{(B)})/\log_{10}(100) = 1/2 \log_{10}(c_1^{(B)}/c_2^{(B)})$ as predicted by Eq. (30).

V. SUMMARY AND DISCUSSION

In a minimalist model of channel transport of two species between two baths, we investigated how interspecies cooperation and competition depend on the entanglement of the respective transport properties. Transition dynamics between channel states were described as a Markov process in a nine-dimensional state space, which in contrast to mean-field approaches conserves interspatial correlations of interparticle interactions. The graphic visualization of the occupation probability of states and flows between them reveals the preferred paths in state space, the degree to which transports of the two species are entangled, and the implication of the latter on local entropy production within the state space. In addition, it shows how global parameters as particle flow between baths or mixing entropy production arise from their local counterpart.

The entanglement of the transport of the species was varied by increasing the affinity of the empty channel to absorb any particle and a repulsive intraspecies interaction, which hampers occupation of the channel by particles of the same species. This procedure favors occupation of the channel by single particles of any species, and by two particles of different species, which couples the transport of the two species. With increasing coupling, the transition dynamics is almost confined to a cyclic sub-space (CS (19)) within the state space. Here, the perfect coupling of the two-species transport causes their particle flows to be equivalent. For parallel concentration gradients of the species it was shown that towards this limiting case the capability of the system for cooperation increases. This implied that mutual flow of either species increased with increasing gradient of the other species. The situation is different when the coupling strength increases for opposing concentration gradients. For loose coupling they drive their species rather independently from each other through the channel. Direction of flow and concentration gradient are parallel, and, hence, the mixing entropy production of both is positive. With increasing coupling strength, the magnitude of flow of the driving species, i.e., that under the influence of the stronger thermodynamic driving force, decreases; however, direction of flow and concentration gradient remain parallel and the corresponding entropy production stays positive. Flow of the driven species shifts towards that of the driving one, and eventually flow direction changes sign and becomes antiparallel to its concentration gradient. Hence, its production of mixing entropy becomes negative. An increase of the coupling strength is also reflected by the increase of effectiveness, i.e., of the amount of negative entropy production of the driven species per positive entropy production of the driving on. In this context we could demonstrate how these productions of mixing entropy of the two species originate from entropy productions related to transitions in state space, i.e., the latter are the sources of the former.

Particle transport through (nano) channels, which connect two baths, has been extensively worked on in the past. Focus was laid primarily on the impact of particle-channel interaction. For particles which do not interact, flow is proportional to the translocation probability, i.e., the probability that a particle located at one channel end leaves it at the other [13]. For fast exchange dynamics at the channel ends, this conditional probability is proportional to $\langle \exp(\Phi(x))/D(x) \rangle^{-1}$, where $\langle \bullet \rangle$ denotes the spatial average along the channel, $D(x)$ is the diffusion coefficient, and Φ is the particle-channel interaction potential, or more general free energy, when entropic forces are also included [14–16]. This implies that, for noninteracting particles, flow is independent of spatial permutations of the particle-channel interaction, e.g., independent from the location of an attractive binding site. Additionally flow monotonically increases for attractive interactions [$\Phi(x) < 0$].

The situation changes when a particle inside the channel impedes access of those from the baths. Flow is then the product of flow, which would be present in the absence of

interparticle interaction, and the probability to find the channel nonoccupied [17,18]. The latter decreases with increasing binding strength of the channel, i.e., it exhibits an opposed dependence compared with that of the flow in the absence of interparticle interaction. So there is a trade-off, i.e., an optimum binding strength, for which flow reaches a maximum [15,17–20]. This holds for sufficient low particle concentrations or fast exchange dynamics at the channel ends. However, this optimum binding strength may, for very high particle concentrations, or slow exchange dynamics of particles at the channel ends, even be repulsive [16,20].

The direction of a concentration gradient asymmetrically affects the probability to find a location inside the channel nonoccupied. So it is lower for a binding site which is located near the bath with the higher concentration when compared to its symmetric counterpart located near the bath with the lower concentration. Hence, a binding site located at the trans position of the concentration gradient implies a higher flow than that in the cis position [15,19]. This flux asymmetry also holds when entropic forces bind the particle [21].

The above model, which allows only one particle to occupy the channel, was applied to study the effect of interparticle interaction for two-species transport [16]. In this model the interparticle interaction of a particle inside the channel is restricted to blocking access of other particles from the baths to the channel. So, selectivity in transport may only be achieved when the two species differ by transport properties or particle-channel interactions. For example, a binding site of one species may favor its transport at the cost of the other, which has no attractive particle-channel interaction. However, this selectivity is based on pure competition, i.e., transport of any species would be higher in the absence of the concentration gradient of the other.

When interparticle interactions are also feasible within the channel, a variety of new effects related to cooperation and competition appear which were addressed by mean-field approaches and simulations [22–24]. In contrast to the aforementioned mean-field approaches, exactly solvable Markovian models do explicitly conserve spatial correlations between channel sites [4–6], and therefore provide even deeper insights into the coupling of two species transport. For oppositely directed concentration gradients it was shown that this coupling could be increased by elongation of the channel and appropriate particle-channel interactions, so that one species could drive the other against its concentration gradient [4,5]. We could show that species, which are under the influence of parallel directed concentration gradients, may cooperate, they may mutually promote the other species at the cost of its own, or they may completely compete for transport [6]. Which kind of regime is present depends, among others, on the concentration gradients in the baths and the strength of particle channel interactions. Competition in the presence of parallel concentration gradients means that flow of each species is lower compared with that in the absence of the other's gradient. This may be easily explained by jamming, following the same arguments as for the channel blocking discussed above. The other regimes demand more sophisticated explanations. One species may promote another, as its own concentration gradient implies an asymmetric occupation of the channel locations and, hence, an asymmetric sterical interaction profile for the other species within the channel. These asymmetric constraints act as an entropic force which biases flow of the other species in the direction of the gradient. If this bias is stronger than blocking, then the gradient increases flow of the other species. This effect was also shown by simulations [23]. Finally, the regime of cooperation means, that the effect of promotion is mutually given for both species. We also found that a longer channel is more capable for cooperation and promotion as it offers more spatial options for particles of different species to interact [6].

In this paper now, we directly focused on the in-channel interparticle interaction and its implication for two-species particle flow. This was done in the shortest possible channel which allows interparticle interaction inside, namely a channel with two occupation sites. The simple structure of state space and transitions within made it easy to identify interactions, which confine stochastic transitions in state space to a cyclic path, on which transport of both species is optimally coupled, by making the thermodynamic driving forces act in series. This made the capability for cooperation in the case of parallel concentration gradients increase. In contrast, in the case of antiparallel concentration gradients, optimum coupling amplifies the effectiveness that one species drives the other against its concentration gradient. Though the nine-dimensional-state space appears simple, its relation with the nonconservative thermodynamic driving forces acting within still offers many issues which have to be addressed. Besides the CS, on which the transition dynamics implies perfect transport coupling of the two species, there are other cyclic paths in which free energy is gained. These "leak" flows in state space demand further evaluation. Another question is whether there are, perhaps exotic, transition-interaction patterns in state space, for which far from equilibrium an increase of the gradient of one species implies a reduction in its flow, i.e., the thermodynamic response acts opposite to its direction of force like a Brownian donkey.

ACKNOWLEDGMENTS

The authors thanks his mentor, Walter Nadler [Institute for Advanced Simulation (IAS), Juelich Supercomputing Centre (JSC), Forschungszentrum Juelich, D-52725 Jülich, Germany], for his always-stimulating, -imaginative, and -visionary discussions and support. The author's research was supported by the Deutsche Forschungsgemeinschaft (Grants No. SFB 688 and No. TP B05) and the Bundesministerium für Bildung und Forschnung (Grant No. BMBF01 EO1504).

APPENDIX A: FLOW IN CYCLIC STATE SPACE

In order to derive Eq. (21), we do not start with a cyclic state space but with an open linear one, which has N positions, the ends of which (position 1 and N) are adjacent to reservoirs (baths), which we label 0 and $N+1$, respectively. Within the state space stochastic transitions are only allowed between neighboring positions, and, at the ends, also with the reservoirs. The dynamics is that of an stationary Markov process. Though this model holds for any Markovian transition dynamics between states, it is simpler for our understanding to consider the positions as spatial

ones and the interaction at the ends with the reservoirs as particle exchange processes. The reservoirs serve as a constant source with concentrations P_0, P_{N+1}, as well as absorbers of particles. Hop-in and -out rates from the reservoirs are $\lambda_{1,0}P_0$, $\lambda_{0,1}$ and $\lambda_{N,N+1}P_{N+1}$, $\lambda_{N+1,N}$. Transitions between states $i \leftarrow j$, $i \neq j$ are given by rates $\lambda_{i\leftarrow j} = \lambda_{i,j}$. So the dynamics of the probability distribution $\boldsymbol{P} = (P_1, \cdots, P_n)^t$ in this state space is determined by

$$\frac{d}{dt}\,\boldsymbol{P} = \boldsymbol{\lambda}\boldsymbol{P} + \begin{pmatrix} \lambda_{1,0}\,P_0 \\ 0 \\ \vdots \\ 0 \\ \lambda_{N,N+1}\,P_{N+1} \end{pmatrix} \tag{A1}$$

with

$$\boldsymbol{\lambda} = \begin{pmatrix} -\lambda_{2,1} - \lambda_{0,1} & \lambda_{1,2} & \cdots & 0 \\ \lambda_{2,1} & -\lambda_{1,2} - \lambda_{3,2} & \cdots & 0 \\ 0 & \lambda_{3,2} & \cdots & 0 \\ & & \vdots & \\ 0 & 0 & \vdots & \lambda_{N-1,N} \\ 0 & 0 & \cdots & -\lambda_{N-1,N} - \lambda_{N+1,N} \end{pmatrix}. \tag{A2}$$

This transition matrix conserves the probability of finding a particle within the channel, $\sum_i \lambda_{i,j} = 0$, except at the ends where transitions to the reservoirs are present. The transition rates define a free-energy difference between respective states $\epsilon_{i+1,i} = -\ln(\lambda_{i+1,i}/\lambda_{i,i+1})$. In the open linear topology of state space they can be derived from a potential, $\epsilon_{i+1,i} = \varphi_{i+1} - \varphi_i$, with $\varphi_j = \sum_{\nu=1}^{j} \epsilon_{\nu,\nu-1} + \varphi_0$. The potential of reservoir "0," φ_0, may be set arbitrary. This implies a potential difference between the reservoirs

$$\Delta U = \varphi_{N+1} - \varphi_0 = \sum_{\nu=1}^{N+1} \epsilon_{\nu,\nu-1} = -\ln\left(\prod_{\nu=1}^{N+1} \frac{\lambda_{\nu,\nu-1}}{\lambda_{\nu-1,\nu}}\right). \tag{A3}$$

Flow between neighboring states $J_{i+1\leftarrow i} = J_{i+1,i}$ is given by

$$J_{i+1,i} = \lambda_{i+1,i}\,P_i - \lambda_{i,i+1}P_{i+1}. \tag{A4}$$

It is convenient to rewrite the transition rates between neighboring states in terms of potentials,

$$\begin{aligned} \lambda_{i+1,i} &= \bar{\lambda}_{i+1} e^{-(\varphi_{i+1}-\varphi_i)/2} \\ \lambda_{i,i+1} &= \bar{\lambda}_{i+1} e^{-(\varphi_i-\varphi_{i+1})/2}, \quad \text{with} \quad \bar{\lambda}_{i+1} = \sqrt{\lambda_{i+1,i}\lambda_{i,i+1}} \end{aligned} \tag{A5}$$

as a measure of mobility between the states. This enables us to write flow between states in terms of activities a_i and resistances R_i. With $\bar{\varphi}_{i+1} = 1/2(\varphi_{i+1} + \varphi_i)$ as the mean potential of two nearby states we get

$$\underbrace{e^{\varphi_i}\,P_i}_{=a_i} - \underbrace{e^{\varphi_{i+1}}\,P_{i+1}}_{=a_{i+1}} = J_{i+1,i}\,\underbrace{\frac{e^{\bar{\varphi}_{i+1}}}{\bar{\lambda}_{i+1}}}_{=R_{i+1}}. \tag{A6}$$

In the steady state, flow is constant throughout, $J_{i+1,i} \equiv J$. Adding the activity differences in Eq. (A6) flow results in the form of an Ohm's law,

$$a_0 - a_{N+1} = J\sum_{i=1}^{N+1} R_i. \tag{A7}$$

However, a cyclic state space demands a more sophisticated approach, since, as we will see, the baths will be integrated into state space. It was recently shown that for unidirectional transport, i.e., concentration in one bath vanishes (symbolized by the subscript "$0 \rightarrow N+1$" for $P_{N+1} = 0$, or labeled by subscript "$0 \leftarrow N+1$" for $P_0 = 0$), the steady-state flow fulfills [25]

$$J_{0\rightarrow N+1} = \mathcal{N}_{1\rightarrow N+1}/\tau_{1\rightarrow N+1}, \tag{A8}$$

$$J_{0\leftarrow N+1} = -\mathcal{N}_{0\leftarrow N}/\tau_{0\leftarrow N}, \tag{A9}$$

with $\tau_{1\rightarrow N+1}$ as the mean first passage time of a particle which starts at positions $i = 1$, is reflected when trying to jump back to bath 0 and which is completely absorbed in bath $N+1$. The opposite conditions holds for $\tau_{0\leftarrow N}$. It is noteworthy that this relation describes a situation in which both ends of state space are in exchange with the reservoirs; however, the mean first passage times derive from a setup with reflective boundary conditions, which also explains our different choice of index for the first passage times, i.e., $1 \rightarrow N+1$ when compared to that of flow $0 \rightarrow N+1$ and vice versa in the other direction. $\mathcal{N}$ is the number of particles within the state space, i.e., $\mathcal{N} = \sum_{i=1}^{N} P_i^{(s)}$ for either direction. These $P_i^{(s)}$ in the steady state are determined from Eq. (A1) by setting $\dot{\boldsymbol{P}} = 0$, i.e.,

$$\boldsymbol{P}^{(s)}_{0\rightarrow N+1} = \boldsymbol{\lambda}^{-1}\begin{pmatrix} \lambda_{1,0}\,P_0 \\ 0 \\ \vdots \\ 0 \end{pmatrix} \text{ or}$$

$$\boldsymbol{P}^{(s)}_{0\leftarrow N+1} = \boldsymbol{\lambda}^{-1}\begin{pmatrix} 0 \\ \vdots \\ 0 \\ \lambda_{N,N+1}\,P_{N+1} \end{pmatrix}. \tag{A10}$$

Hence, these particle numbers are proportional to the respective concentrations in the reservoirs, $\mathcal{N}_{1\rightarrow N+1} \sim P_0$ and $\mathcal{N}_{0\leftarrow N} \sim P_{N+1}$. This suggests introducing specific particle

numbers n, which is independent from the bath activities. This is achieved by normalizing the particle number by the respective activities [14–16], i.e., with

$$n_{1\to N+1} = \frac{\mathcal{N}_{1\to N+1}}{e^{\varphi_0} P_0}, \quad n_{0\leftarrow N} = \frac{\mathcal{N}_{0\leftarrow N}}{e^{\varphi_{N+1}} P_{N+1}}, \tag{A11}$$

we get

$$J_{0\to N+1} = a_0 \quad n_{1\to N+1}/\tau_{1\to N+1}, \tag{A12}$$

$$J_{0\leftarrow N+1} = -a_{N+1} n_{0\leftarrow N}/\tau_{0\leftarrow N}. \tag{A13}$$

For arbitrary concentrations in the baths, steady-state flow is the superposition of the two unidirectional flows above. In particular, as flow vanishes for equal activities in the baths, we obtain

$$\frac{n_{1\to N+1}}{\tau_{1\to N+1}} = \frac{n_{0\leftarrow N}}{\tau_{0\leftarrow N}} = \frac{n}{\tau}, \tag{A14}$$

where $n = 1/2(n_{1\to N+1} + n_{0\leftarrow N})$ and $\tau = 1/2(\tau_{1\to N+1} + \tau_{0\leftarrow N})$ are the symmetrical specific particle number and first passage time. So steady-state flow for arbitrary concentrations in the baths takes the form

$$J = \frac{n}{\tau}(a_0 - a_{N+1}). \tag{A15}$$

Note that with Eqs. (A6) and (A7) n/τ is the conductivity (inverse of resistance R)

$$n/\tau = R^{-1} = \left(\sum_{i=1}^{N+1} R_i\right)^{-1} = \left(\sum_{i=1}^{N+1} \frac{e^{\bar{\varphi}_i}}{\bar{\lambda}_i}\right)^{-1}. \tag{A16}$$

The explicit determination of the mean first passage times is a bit tedious and can be looked up in Refs. [9,26]. In short, one modifies the transition matrix in Eq. (A2), $\boldsymbol{\lambda} \to \boldsymbol{\lambda}'$, so that there are either reflective boundary conditions towards bath 0 for determination of $\tau_{1\to N+1}$ and, vice versa, towards bath $N+1$ when $\tau_{0\leftarrow N}$ is considered. This is accomplished by just taking out the appropriate hop-out rates. For determination of $\tau_{1\to N+1}$ one positions a particle at $i = 1$ and lets the system evolve, i.e., $\boldsymbol{P}(t) = \exp(\boldsymbol{\lambda}' t)\boldsymbol{e}_1$, with $\boldsymbol{e}_1 = (1,0,\ldots,0)^t$. The mean first passage time is defined as the mean time the particle needs to get absorbed in bath $N+1$. So $\tau_{1\to N+1} = \int_0^\infty dt\ t\ (-dp(t)/dt) = \int_0^\infty dt\ p(t)$, where $p(t) = (1,1\cdots,1)\boldsymbol{P}(t) = \sum_{i=1}^N P_i(t)$ is the probability to find the particle still in state space, i.e., $-dp(t)/dt$ is the fraction absorbed at t by bath $N+1$. So one gets

$$\tau_{1\to N+1} = (1,1\cdots,1)\frac{1}{\boldsymbol{\lambda}'}\boldsymbol{e}_1 = \boldsymbol{e}_1^t \frac{1}{(\boldsymbol{\lambda}')^t}\begin{pmatrix}1\\1\\\vdots\\1\end{pmatrix}. \tag{A17}$$

The same holds for $\tau_{0\leftarrow N}$. The above matrix equation may be solved directly and we get for the mean first passage times

$$\tau_{1\to N+1} = \sum_{i=1}^{N+1}\sum_{\nu=1}^{N} e^{-\varphi_\nu}\frac{e^{\bar{\varphi}_i}}{\bar{\lambda}_i}\,\theta(i-\nu-1), \tag{A18}$$

$$\tau_{0\leftarrow N} = \sum_{i=1}^{N}\sum_{\nu=1}^{N} e^{-\varphi_\nu}\frac{e^{\bar{\varphi}_i}}{\bar{\lambda}_i}\,\theta(\nu-i), \tag{A19}$$

$$\tau = \frac{1}{2}\left(\sum_{\nu=1}^{N} e^{-\varphi_\nu}\right)\left(\sum_{i=1}^{N+1}\frac{e^{\bar{\varphi}_i}}{\bar{\lambda}_i}\right), \tag{A20}$$

where $\theta(x)$ is the unit step function, with $\theta = 0$, for $x < 0$ and otherwise $\theta = 1$. Note that the above equations are well known in integral form for continuous diffusion-reaction processes (e.g., Ref. [26]) and look similar. However, results cannot be transferred readily to the discrete case as details, e.g., the distinction between the potential φ_i of a state i and the mean potential between two states $\bar{\varphi}_i$, appear only in the discrete case, whereas both become equivalent in the continuum limit.

Now we have the tools to tackle the cyclic state space. In the steady state we can modify the model of a linear state space between two reservoirs to a cyclic state space by adding one position, namely that of bath 0 and closing the bath positions 0 and $N+1$ together so that we end up with a ringlike state space with $N+1$ positions $0, 1\cdots N$. This implies that $P_0 = P_{N+1}$. One round in this cyclic space implies that the free-energy change is ΔU [see Eq. (A3)]. Note that the ring topology impedes to define a unique potential from free-energy differences, as continuation would imply $\varphi_{N+1} = \varphi_0 + \Delta U \neq \varphi_0$. As the off-set potential may be chosen arbitrarily, we set it equal to zero, i.e., $\varphi_0 = 0$. So, with Eq. (A15), flow in this cyclic space becomes

$$J = \frac{n}{\tau} P_0(1 - e^{\Delta U}). \tag{A21}$$

In contrast to the open situation between two baths, we now have a closed system, and conservation of probability holds, $\sum_{i=0}^N P_i = 1$. According to Eq. (A11), we get the constraint

$$\begin{aligned} 1 &\stackrel{!}{=} P_0 + \mathcal{N}_{1\to N+1} + \mathcal{N}_{0\leftarrow N} \\ &= P_0(1 + n_{1\to N+1} + n_{0\leftarrow N} e^{\Delta U}). \end{aligned} \tag{A22}$$

Insertion into Eq. (A21) and considering Eq. (A14) then gives for the steady-state flow in a cyclic space

$$J = \frac{1 - e^{\Delta U}}{\tau_{1\to N+1} + \tau_{0\leftarrow N}\ e^{\Delta U} + \tau/n}. \tag{A23}$$

Inserting the first passage times from Eqs. (A20) and the resistance from Eq. (A16) finally allows us to determine flow according to Eq. (21).

APPENDIX B: COOPERATION AND COMPETITION IN CYCLIC STATE SPACE

To investigate the features of the cyclic state space for cooperation and competition, e.g., when the concentration of one species is enhanced, we pick one transition between two states $j \leftarrow j-1$ within the cycle and increase the rate in the counterclockwise direction by a factor $\alpha > 1$,

$$\lambda'_{j,j-1} = \alpha\lambda_{j,j-1}\ . \tag{B1}$$

This can, for example, be accomplished by an increase of particle concentration, $k_+ c \to k_+ c'$ with $c' > c$, i.e., $\alpha = c'/c$. The backward rate $\lambda_{j-1,j}$ shall remain unchanged. This implies a change in potentials and mobilities. With

$$\delta\varphi = -\ln(\alpha) < 0 \tag{B2}$$

we get

$$\varphi'_i = \begin{cases}\varphi_i, & i < j\\ \varphi_i + \delta\varphi, & i \geqslant j\end{cases},$$

in particular the free-energy difference after one round in the cyclic state space changes to

$$\Delta U' = \varphi'_{N+1} - \varphi'_0 = \Delta U + \delta\varphi.$$

Potentials between states change to

$$\bar{\varphi}'_i = \begin{cases} \bar{\varphi}_i, & i < j \\ \bar{\varphi}_j + \delta\varphi/2, & i = j \\ \bar{\varphi}_i + \delta\varphi, & i > j \end{cases},$$

and mobilities to

$$\bar{\lambda}'_i = \begin{cases} \bar{\lambda}_j \ \sqrt{\alpha} = \bar{\lambda}_j e^{\delta\varphi/2}, & i = j \\ \bar{\lambda}_i & \text{else} \end{cases}. \tag{B3}$$

We will investigate how this effects first passage times and by this flow in Eq. (A23). After explicit evaluation of the unit step function θ we derive from Eqs. (A20)

$$\tau'_{1\to N+1} = \sum_{\substack{i=2 \\ i\neq j}}^{N+1} \sum_{\nu=1}^{i-1} \frac{e^{\bar{\varphi}'_i}}{\bar{\lambda}'_i} e^{-\varphi'_\nu} + \underbrace{\frac{e^{\bar{\varphi}'_j}}{\bar{\lambda}'_j}}_{=e^{\delta\varphi}\frac{e^{\bar{\varphi}_j}}{\bar{\lambda}_j}} \sum_{\nu=1}^{j-1} e^{-\varphi'_\nu}$$

$$= \sum_{i=2}^{N+1} \sum_{\nu=1}^{i-1} \frac{e^{\bar{\varphi}_i}}{\bar{\lambda}_i} e^{-\varphi_\nu} e^{\delta\varphi\ \theta(j-\nu-1)\theta(i-j)}. \tag{B4}$$

As $e^{\delta\varphi} < 1$, the inequality

$$e^{\delta\varphi}\tau_{1\to N+1} < \tau'_{1\to N+1} < \tau_{1\to N+1} \tag{B5}$$

holds, i.e., the first passage time in direction $1 \to N+1$ becomes shorter; however, it is still longer than a lower boundary given by the factor $e^{\delta\varphi}$. Similarly, one can show for the first passage time in the opposite direction

$$\tau'_{0\leftarrow N} = \sum_{i=1}^{N} \sum_{\nu=i}^{N} \frac{e^{\bar{\varphi}_i}}{\bar{\lambda}_i} e^{-\varphi_\nu} e^{-\delta\varphi\ \theta(\nu-j)\theta(j-i-1)}, \tag{B6}$$

i.e.,

$$e^{-\delta\varphi}\tau_{0\leftarrow N} > \tau'_{0\leftarrow N} > \tau_{0\leftarrow N}. \tag{B7}$$

For the resistance [Eq. (A16)] one gets

$$(\tau/n)' = \sum_{i=1}^{N} \frac{e^{\bar{\varphi}_i}}{\bar{\lambda}_i} e^{\delta\varphi\theta(i-j)}, \tag{B8}$$

i.e.,

$$e^{\delta\varphi}(\tau/n) < (\tau/n)' < (\tau/n). \tag{B9}$$

Two constellations are now of interest. First, we assume that the rate we increase by elevation of the related particle concentration points parallel to the flow direction on the cyclic state space. So flow points in the counterclockwise direction, and $\Delta U < 0$, which implies

$$J' = \frac{1 - e^{\Delta U'}}{\tau'_{1\to N+1} + \tau'_{0\leftarrow N}\ e^{\Delta U'} + (\tau/n)'}$$

$$> \frac{1 - e^{\Delta U}}{\tau_{1\to N+1} + \tau_{0\leftarrow N}\ e^{\Delta U} + (\tau/n)} = J. \tag{B10}$$

This implies that any increase in rate by elevation of the concentration of one partner in direction of flow elevates flow in cyclic state space. As flows of both species are identical in CS, this implies perfect cooperation over the whole range of concentrations.

In contrast, we have the situation when flow on the cyclic state space directs in clockwise orientation, i.e., antiparallel to the direction of the rate we increase by elevation of particle concentration. This implies $J < 0$, and, hence, $\Delta U > 0$ [see Eq. (A23)]. We choose the magnitude of $\delta\varphi$ small enough so that flow J' preserves its negative sign, i.e., $\Delta U' = \Delta U + \delta\varphi > 0$. For the denominator in Eq. (A23) the inequalities (B5), (B7), and (B9) imply

$$\frac{1}{\tau'_{1\to N+1} + \tau'_{0\leftarrow N}\ e^{\Delta U'} + (\tau/n)'} < \frac{e^{-\delta\varphi}}{\tau_{1\to N+1} + \tau_{0\leftarrow N}\ e^{\Delta U} + (\tau/n)}. \tag{B11}$$

Multiplying with $1 - e^{U'}$ (note as its sign is negative the greater-than-sign changes changes its direction) leads to

$$J' = \frac{1 - e^{U'}}{\tau'_{1\to N+1} + \tau'_{0\leftarrow N}\ e^{\Delta U'} + (\tau/n)'}$$

$$> \frac{e^{-\delta\varphi} - e^{\Delta U}}{\tau_{1\to N+1} + \tau_{0\leftarrow N}\ e^{\Delta U} + (\tau/n)}$$

$$> \frac{1 - e^{\Delta U}}{\tau_{1\to N+1} + \tau_{0\leftarrow N}\ e^{\Delta U} + (\tau/n)} = J. \tag{B12}$$

So the anti-parallel-directed increase of rate increases the negative flow towards zero, i.e., it decreases its magnitude. In summary, we demonstrated that an isolated increase of rate, in our model by elevation of the appropriate particle concentration, in the cyclic state space implies a higher magnitude of flow when this rate points in direction of flow, and, vice versa, magnitude of flow is decreased when rate and flow are antiparallel.

APPENDIX C: ENTROPY PRODUCTION AND ITS SOURCES IN STATE SPACE

In this section we will show that the sum over all entropy productions in state space in the steady state

$$\dot{S} = \frac{1}{2} \sum_{\boldsymbol{\sigma},\boldsymbol{\varsigma}\in\boldsymbol{\Sigma}} \dot{S}_{\boldsymbol{\sigma},\boldsymbol{\varsigma}} \tag{C1}$$

is that of mixing entropy production in the baths; or, vice versa, the sources of entropy production by mixing of particles by channel transport may be allocated to that in state space.

For the further evaluation of the sum in Eq. (C1), we separately consider transitions which are involved in particle exchange between bath 1 and the adjacent right channel end, i.e., for species X, $(s,0) \rightleftharpoons (s,X)$, with $s = A,\ B,\ 0$. The corresponding free-energy difference [Eq. (7)] may be written as

$$\Delta\epsilon_{\boldsymbol{\sigma},\boldsymbol{\varsigma}} = -\operatorname{sgn}(\boldsymbol{\sigma},\boldsymbol{\varsigma}) \ln\left[\frac{k_+ c_1^{(X)}}{k_-}\right]$$

$$= \operatorname{sgn}(\boldsymbol{\sigma},\boldsymbol{\varsigma})\left\{-\ln\left[\frac{k_+ c_2^{(X)}}{k_-}\right] - \ln\left[\frac{c_1^{(X)}}{c_2^{(X)}}\right]\right\}$$

$$= \Delta\epsilon^{(e)}_{\boldsymbol{\sigma},\boldsymbol{\varsigma}} - \Delta\mu^{(X)} \operatorname{sgn}(\boldsymbol{\sigma},\boldsymbol{\varsigma}). \tag{C2}$$

The function "sgn" adjusts the sign of the free-energy difference to the sequence of its states in its index. It is $\mathrm{sgn}(\sigma,\varsigma)=1$ when particles enter the channel from bath 1, $\sigma=(s,X)\leftarrow\varsigma=(s,0)$, and, vice versa, $\mathrm{sgn}(\sigma,\varsigma)=-1$ when they leave, $\varsigma=(s,X)\rightarrow\sigma=(s,0)$. According to Eq. (C2) the free-energy difference between states $\boldsymbol{\sigma},\boldsymbol{\varsigma}$ is that that would be present under equilibrium conditions, $\Delta\epsilon^{(e)}_{\boldsymbol{\sigma},\boldsymbol{\varsigma}}$, i.e., when concentrations in both baths equal $c_2^{(X)}$, diminished by the difference of chemical potentials between both baths. All other transitions, and, hence, corresponding free-energy differences, between states which are not involved in particle exchange with bath 1 do not differ from their value under equilibrium conditions. Under equilibrium conditions the states may be assigned a potential $\phi_{\boldsymbol{\sigma}}$ [Eq. (11)], the differences of which determine the free-energy difference between the states [Eq. (12)]. Free-energy differences between states involved in particle transport with bath 1 have to be adjusted by the difference of the chemical potential. Inserting this into Eq. (27) enables us to rewrite the entropy production in Eq. (C1) as

$$\begin{aligned}\dot{S}&=\frac{1}{2}\sum_{\text{with bath 1}}\left(-\Delta\epsilon^{(e)}_{\boldsymbol{\sigma},\boldsymbol{\varsigma}}+\mathrm{sgn}(\boldsymbol{\sigma},\boldsymbol{\varsigma})\Delta\mu^{(X)}\right)J_{\boldsymbol{\sigma},\boldsymbol{\varsigma}}\\&\quad+\frac{1}{2}\sum_{\text{not with bath 1}}-\Delta\epsilon^{(e)}_{\boldsymbol{\sigma},\boldsymbol{\varsigma}}\,J_{\boldsymbol{\sigma},\boldsymbol{\varsigma}}\\&=\frac{1}{2}\sum_{\text{with bath 1}}\Delta\mu^{(X)}\,\mathrm{sgn}(\boldsymbol{\sigma},\boldsymbol{\varsigma})\,J_{\boldsymbol{\sigma},\boldsymbol{\varsigma}}\\&\quad+\frac{1}{2}\left(\sum_{\text{with bath 1}}(-\phi_{\boldsymbol{\sigma}}+\phi_{\boldsymbol{\varsigma}})\,J_{\boldsymbol{\sigma},\boldsymbol{\varsigma}}\right.\\&\quad\left.+\sum_{\text{not with bath 1}}(-\phi_{\boldsymbol{\sigma}}+\phi_{\boldsymbol{\varsigma}})\,J_{\boldsymbol{\sigma},\boldsymbol{\varsigma}}\right)\\&=\frac{1}{2}\sum_{\text{with bath 1}}\Delta\mu^{(X)}\,\mathrm{sgn}(\boldsymbol{\sigma},\boldsymbol{\varsigma})\,J_{\boldsymbol{\sigma},\boldsymbol{\varsigma}}\\&\quad+\frac{1}{2}\sum_{\boldsymbol{\sigma},\boldsymbol{\varsigma}\in\boldsymbol{\Sigma}}(-\phi_{\boldsymbol{\sigma}}+\phi_{\boldsymbol{\varsigma}})\,J_{\boldsymbol{\sigma},\boldsymbol{\varsigma}}\,.\end{aligned}\tag{C3}$$

The latter terms vanish as in the steady-state flow is conserved around a state [Kirchoff's circuit rule, see Eq. (15)], i.e.,

$$\sum_{\boldsymbol{\sigma},\boldsymbol{\varsigma}\in\boldsymbol{\Sigma}}\phi_{\boldsymbol{\sigma}}\,J_{\boldsymbol{\sigma},\boldsymbol{\varsigma}}=\sum_{\boldsymbol{\sigma}\in\boldsymbol{\Sigma}}\phi_{\boldsymbol{\sigma}}\underbrace{\sum_{\boldsymbol{\varsigma}\in\boldsymbol{\Sigma}}J_{\boldsymbol{\sigma},\boldsymbol{\varsigma}}}_{=0}=0.\tag{C4}$$

Note that the same is true for $\sum_{\boldsymbol{\sigma},\boldsymbol{\varsigma}\in\boldsymbol{\Sigma}}\phi_{\boldsymbol{\varsigma}}\,J_{\boldsymbol{\sigma},\boldsymbol{\varsigma}}$, as $J_{\boldsymbol{\sigma},\boldsymbol{\varsigma}}=-J_{\boldsymbol{\varsigma},\boldsymbol{\sigma}}$. The flows in the first term of Eq. (C3) consist of those for species A and B,

$$\begin{aligned}&\frac{1}{2}\sum_{\text{with bath 1}}\Delta\mu^{(X)}\,J_{\boldsymbol{\sigma},\boldsymbol{\varsigma}}\\&\quad=\Delta\mu^{(A)}\frac{1}{2}\sum_{A\text{ with bath 1}}\mathrm{sgn}(\boldsymbol{\sigma},\boldsymbol{\varsigma})J_{\boldsymbol{\sigma},\boldsymbol{\varsigma}}\\&\qquad+\Delta\mu^{(B)}\frac{1}{2}\sum_{B\text{ with bath 1}}\mathrm{sgn}(\boldsymbol{\sigma},\boldsymbol{\varsigma})J_{\boldsymbol{\sigma},\boldsymbol{\varsigma}}.\end{aligned}$$

The sum over the particle exchange flows at the channel ends is just twice the steady-state flow $J^{(A)}$, $J^{(B)}$ of the respective species between the baths [see Eq. (17)]. Finally, we get for the entropy production

$$\dot{S}=\Delta\mu^{(A)}J^{(A)}+\Delta\mu^{(B)}J^{(B)}.\tag{C5}$$

This equation states that the sum over the particular entropy productions in state space is that of the mixing entropy production in the baths. Conversely, this equation states that the sources of the overall mixing entropy production may be allocated to those in state space.

[1] S. M. Iqbal, D. Akin, and R. Bashir, Nat. Nanotechnol. **2**, 243 (2007).

[2] T. Jovanovic-Talisman, J. Tetenbaum-Novatt, A. S. McKenney, A. Zilman, R. Peters, M. P. Rout, and B. T. Chait, Nature **457**, 1023 (2009).

[3] T. Chou, Phys. Rev. Lett. **80**, 85 (1998).

[4] T. Chou, J. Chem. Phys. **110**, 606 (1999).

[5] T. Chou and D. Lohse, Phys. Rev. Lett. **82**, 3552 (1999).

[6] W. R. Bauer and W. Nadler, Phys. Rev. E **88**, 010703 (2013).

[7] We consider the gain of free energy as the negative of the corresponding free-energy difference $\Delta\epsilon$ between the baths, i.e., in this case $\Delta\epsilon=-\Delta\mu$.

[8] Note that we normalize all energetic quantities to kT, i.e., $\Phi\rightarrow\Phi/kT$, with k as the Boltzmann constant and T as the temperature.

[9] W. Nadler and K. Schulten, J. Chem. Phys. **84**, 4015 (1986).

[10] We notate the sequence of state variables of a transition $\boldsymbol{\sigma}\leftarrow\boldsymbol{\varsigma}$ as $\boldsymbol{\sigma},\boldsymbol{\varsigma}$ in the index of the transition rate λ to be in line with the usual index notation in matrix algebra.

[11] For counterclockwise (clockwise) direction select the state $\boldsymbol{\sigma}_{i+1}$ ($\boldsymbol{\sigma}_{i-1}$) as a start and impede transitions from this state in clockwise (counterclockwise) direction (reflective boundary conditions). τ_+ (τ_-) is then the mean time to reach $\boldsymbol{\sigma}_i$ for the first time (absorptive boundary conditions).

[12] J. Schnackenberg, Rev. Mod. Phys. **48**, 571 (1976).

[13] A. M. Berezhkovskii, M. A. Pustovoit, and S. M. Bezrukov, J. Chem. Phys. **116**, 9952 (2002); **119**, 3943 (2003).

[14] W. R. Bauer and W. Nadler, J. Chem. Phys. **122**, 244904 (2005).

[15] W. R. Bauer and W. Nadler, Proc. Natl. Acad. Sci. U.S.A. **103**, 11446 (2006).

[16] W. R. Bauer and W. Nadler, PLoSONE **5**, e15160 (2010).

[17] A. M. Berezhkovskii and S. M. Bezrukov, Chem. Phys. **319**, 342 (2005).

[18] A. M. Berezhkovskii and S. M. Bezrukov, Biophys. J. **88**, L17 (2005).

[19] S. M. Bezrukov, A. M. Berezhkovskii, and A. Szabo, J. Chem. Phys. **127**, 115101 (2007).
[20] A. B. Kolomeisky, Phys. Rev. Lett. **98**, 048105 (2007).
[21] A. M. Berezhkovskii, M. A. Pustovoit, and S. M. Bezrukov, Phys. Rev. E **80**, 020904 (2009).
[22] A. Zilman, J. Pearson, and G. Bel, Phys. Rev. Lett. **103**, 128103 (2009).
[23] A. Zilman, S. D. Talia, T. Jovanovic-Talisman, B. T. Chait, M. P. Rout, and M. O. Magnasco, PLoS Comput. Biol. **6**, e1000804 (2010).
[24] A. Zilman and G. Bel, J. Phys.: Condens. Matter **22**, 454130 (2010).
[25] S. L. Hardt, Bull. Math. Biol. **43**, 89 (1981).
[26] W. Nadler and K. Schulten, J. Chem. Phys. **82**, 151 (1985).